Application of Ensemble Empirical Mode Decomposition in Low-Frequency Lightning Electric Field Signal Analysis and Lightning Location

Xiangpeng Fan[®], Yijun Zhang[®], Paul R. Krehbiel, Yang Zhang, Dong Zheng, Wen Yao, Liangtao Xu[®], Hengyi Liu, and Weitao Lyu

Abstract—The application of empirical mode decomposition (EMD) in the analysis and processing of lightning electric field waveforms acquired by the low-frequency e-field detection array (LFEDA) in China has significantly improved the capabilities of the low-frequency/very-low-frequency (LF/VLF) time-of-arrival technique for studying the lightning discharge processes. However, the inherent mode mixing and the endpoint effect of EMD lead to certain problems, such as an inadequate noise reduction capability, the incorrect matching of multistation waveforms, and the inaccurate extraction of pulse information, which limit the further development of the LFEDA's positioning ability. To solve these problems, the advanced ensemble EMD (EEMD) technique is introduced into the analysis of LF/VLF lightning measurements, and a double-sided bidirectional mirror (DBM) extension method is proposed to overcome the endpoint effect of EMD. EEMD can effectively suppress mode mixing, and the DBM extension method proposed in this article can effectively suppress the endpoint effect, thus greatly improving the accuracy of a simulated signal after a 25-500-kHz bandpass filter. The resulting DBM_EEMD algorithm can be used in the

Manuscript received January 9, 2020; revised April 1, 2020; accepted April 27, 2020. This research was supported by the National Key Research and Development Program of China (2017YFC1501501), the National Natural Science Foundation of China (Grants 41875001, 91537209, 41675005, and 41775009), the Basic Research Fund of the Chinese Academy of Meteorological Sciences (Grant 2018Z003), and the National Science Foundation (AGS 1720600). (Corresponding author: Yijun Zhang.)

Xiangpeng Fan is with the Department of Atmospheric and Oceanic Sciences, Fudan University, Shanghai 200438, China, also with the Institute of Atmospheric Sciences, Fudan University, Shanghai 200438, China, and also with the State Key Laboratory of Severe Weather (LASW), Chinese Academy of Meteorological Sciences, Beijing 100081, China (e-mail: fanxp@cma.gov.cn).

Yijun Zhang is with the Department of Atmospheric and Oceanic Sciences, Fudan University, Shanghai 200438, China, also with the Institute of Atmospheric Sciences, Fudan University, Shanghai 200438, China, and also with the CMA-FDU Joint Laboratory of Marine Meteorology, Shanghai 200438, China (e-mail: zhangyijun@fudan.edu.cn).

Yang Zhang, Dong Zheng, Wen Yao, Liangtao Xu, Hengyi Liu, and Weitao Lyu are with the State Key Laboratory of Severe Weather (LASW), Chinese Academy of Meteorological Sciences, Beijing 100081, China (e-mail: zhangyang@cma.gov.cn; zhengdong@cma.gov.cn; yaowen@cma.gov.cn; xult@cma.gov.cn; liuhy@cma.gov.cn; wtlyu@cma.gov.cn).

Paul R. Krehbiel is with the Langmuir Laboratory for Atmospheric Research, Geophysical Research Center, New Mexico Institute of Mining and Technology, Socorro, NM 87801 USA (e-mail: krehbiel@ibis.nmt.edu).

Color versions of one or more of the figures in this article are available online at http://ieeexplore.ieee.org.

Digital Object Identifier 10.1109/TGRS.2020.2991724

LFEDA system to process and analyze the detected electric field signals to improve the system's lightning location capabilities, especially in terms of accurate extraction and location of weak signals from lightning discharges. In this article, a 3-D image of artificially triggered lightning obtained from an LF/VLF location system is reported for the first time, and methods for further improving the location capabilities of the LF/VLF lightning detection systems are discussed.

Index Terms—Double-sided bidirectional mirror (DBM) extension, ensemble empirical mode decomposition (EEMD), lightning location, low-frequency/very-low-frequency (LF/VLF) electric field.

I. INTRODUCTION

THE process of lightning discharge produces electromagnetic radiation over a wide spectrum, which provides an important means of remote sensing detection and location for lightning. Lightning flashes consist of many independent physical processes, each of which produces electric and magnetic fields with certain characteristics [1]–[3]. Considering the differences in the rates and amplitudes of electromagnetic radiation at different frequencies, different lightning detection and location technologies have different capabilities for different physical processes of lightning [4]. In the low-frequency/verylow-frequency (LF/VLF) band, a lightning radiation signal usually has high radiation energy and a long transmission distance, which can be used to detect and locate the large pulses generated by a lightning discharge and to determine the lightning type in accordance with the characteristics of the pulse waveform. For a long time, lightning detection and location systems operating in the LF/VLF band have played an important role in research and applications related to thunderstorm monitoring and early warning, the weather and climate characteristics of lightning, lightning physics, and lightning disaster analysis.

The most widely used lightning location system is the ground flash location system developed by the University of Arizona. It operates in the LF/VLF band of 400 Hz–400 kHz. By virtue of developments in location technology, this location system combined with the time-of-arrival (TOA) location technique can achieve relatively accurate positioning for the

return stroke of a ground flash. Based on this technology, the National Lightning Detection Network (NLDN), consisting of more than 100 stations, was established in the United States, with baseline lengths of 300–350 km [4]–[6]. Many other countries and regions have also subsequently established ground flash positioning systems similar to the NLDN that cover other key areas at either the national or local scale, such as the North American Lightning Detection Network (NALDN) [7]; the Guangdong Lightning Location System (GDLLS) [8], which covers Guangdong Province in China; the Guangdong—Hong Kong—Macau Lightning Location System (GHMLLS), which covers key areas of the Pearl River Delta in China [9]; and the European Cooperation for Lightning Detection (EUCLID) network, which is jointly operated by many countries in Europe [10].

With the further development of lightning detection and location technology, researchers have found that not only can the return stroke pulses of a ground flash be used for location but also other pulse signals generated by lightning discharges can be located. Los Alamos National Laboratory in the United States first developed the Los Alamos Sferic Array (LASA) system for total lightning detection in the LF/VLF frequency band of 200 Hz-500 kHz to realize the three-dimensional positioning of all types of lightning. The station network layout of LASA is based on a cooperative observation scheme that combines long and short baselines; the diameter of the main station network, composed of six stations, is approximately 100 km, whereas the baseline length of the two remaining stations is 200 km [11]–[13]. Subsequently, research institutions in the United States, Germany, Japan, and other countries also developed and built a number of similar detection networks, thus advancing the state of research on thunderstorm electricity and lightning physics. Based on the Huntsville, Alabama Marx Meter Array (HAMMA), with a detection frequency range of 1 Hz-400 kHz, Bitzer et al. [14] successfully located the development processes of single ground flashes and cloud flashes. Through comparisons with the results from the relatively mature North Alabama Lightning Mapping Array (NALMA) and NLDN, it has been found that for the location of lightning development channels, whether for ground flashes or cloud flashes, the results of HAMMA and NALMA match in time and space, and the location information obtained by HAMMA during the initial lightning stage is even richer than that of NALMA. Stolzenburg et al. [15] studied the physical characteristics of natural lightning using the positioning ability of the Position By Fast Antenna (PBFA) system in a working frequency range of 1.6-630 kHz and a high-speed camera. Karunarathne et al. [16] compared the location results for fast electric field changes obtained by this system with the location results of the Lightning Detection and Ranging (LDAR) II system based on very-high-frequency (VHF) signals and found that the LF lightning location system had advantages in terms of capturing the pulse information during the initial lightning stage. At this time, the baseline length between the stations of PBFA was reduced to only tens of kilometers. Yoshida et al. [17] developed a positioning system for the Broadband Observation network for Lightning

and Thunderstorms (BOLT) in Japan. The working frequency range is 800 Hz-500 kHz, and the network is composed of 11 detection antennas. The typical baseline length of each station is 15-25 km from the central station. Under the estimated time measurement error of 200 ns, the location results for lightning pulses can be obtained using the TOA method. The results show that this method has a certain ability to describe the development characteristics of cloud flashes and ground flashes. Wang et al. [18] introduced the multiband Beijing Lightning Network (BLNET), with a coverage of $85 \times 100 \text{ km}^2$, which is composed of 15 stations established in Beijing and the surrounding areas. Based on the location information obtained from the LF lightning electric field pulses, the distribution of lightning activity during a thunderstorm and the development speed, direction, and polarity of initial breakdown were studied for various types of lightning discharges, and the results were consistent with the existing observational conclusions. The working frequency range of the fast antennas in the BLNET system is 1.5 kHz-2 MHz. Lyu et al. [19], [20] developed and built a total lightning positioning system based on LF magnetic field detection, which is called the LF Near-field Interferometric-TOA 3-D Lightning Mapping Array (LFI-LMA). Unlike the above systems, which use lightning electric field pulse signals as the basis for positioning research, the LFI-LMA system detects dB/dt (1-100 kHz) and B (100-250 kHz) in the frequency band of 1-400 kHz, with a sampling rate of 1 MHz. The cross-correlation algorithm is used to calculate the time differences between the arrivals of pulses at different stations. The TOA algorithm is then used to determine the spatial locations and times of the magnetic field pulses to obtain a refined description of lightning channel development. Wu et al. [21] developed a new electric field detection device to improve the positioning capability by improving the device detection performance. The main features of the developed device design are the reduction of the time constant of the antenna to improve the ability to capture the pulse characteristics of a lightning electric field signal, the adoption of a digital acquisition card with a higher sampling frequency and accuracy to improve the detection accuracy, and the capability of continuous collection of electric field signals. On this basis, the Fast Antenna Lightning Mapping Array (FALMA) has been developed, which is an LF/VLF electric field detection system with a significantly improved ability to locate lightning channels.

Through continuous exploration of the applied research methods, as described above, the positioning capabilities of systems based on the LF/VLF lightning signals have been continuously improved. The further development of lightning location capabilities based on LF/VLF lightning electromagnetic field detection is of great significance to lightning physics research. Over time, lightning location capabilities have developed from point to surface to 3-D analysis, from ground lightning location to full lightning location to refined 3-D channel location. The continuous improvements in the positioning capabilities of the LF/VLF lightning detection systems can be attributed to three aspects of development. The first is the optimization of the detection performance of the

detection equipment itself. The second is the improvement of the available electric field signal processing and analysis methods and the development of positioning techniques. Finally, in accordance with the specific purpose of the detection system in combination with the terrain, weather, and climate characteristics, the layout of the station network can be optimized to improve the detection and positioning ability of a particular detection system for lightning electromagnetic fields.

The Low-frequency E-field Detection Array (LFEDA) was built by the Chinese Academy of Meteorological Sciences in 2014. The lightning field detection equipment used in LFEDA consists of rather traditional fast antennas [22]. To monitor lightning discharge activity during large-scale thunderstorms, a multistation detection layout with medium and long baselines is adopted in this system. Shi et al. [23] developed the electric field positioning system based on the technology commonly used in lightning research to give LFEDA the ability to locate lightning discharge pulses and monitor lightning activity during large-scale thunderstorms. Focusing on the development of signal analysis and positioning techniques, Fan et al. [1] introduced the empirical mode decomposition (EMD) algorithm [24] into the analysis of the lightning electric field signals. Combined with the technique of a second cross-correlation process with a reduced window scale, this algorithm can significantly improve the sufficiency of seeking and matching of the pulse signals and the accuracy of pulse peak time extraction based on multistation electric field waveforms [1], [23]. Thus, the lightning location ability of LFEDA has been greatly improved, allowing lightning discharge channels to be described in terms of more radiation sources [1] and playing an important role in the tracing and analysis of a fatal lightning accident [25]. In addition, the research team of LFEDA has explored the potential expansion of the available positioning methods; accordingly, the time reversal (TR) technique has been introduced for threedimensional lightning location [26].

Because EMD filtering is based on an adaptive analysis of the signal characteristics of lightning electric fields and the decomposition filtering of such a signal with the EMD algorithm will not cause a strong phase shift of the signal as a typical filter would [1], the EMD method is very suitable for the analysis of lightning electric fields, the processing of nonlinear and discontinuous signals, and positioning based on multistation lightning electric field measurements. However, it has been found that the inherent mode mixing and the endpoint effect of EMD somewhat restrict the further improvement of LFEDA's lightning location capabilities.

Therefore, this article presents an in-depth analysis of the application of EMD in the lightning electric field signal analysis and attempts to identify effective methods for solving these problems to further improve the positioning performance of the LFEDA system from the perspective of the applied signal analysis and positioning algorithms.

II. LFEDA SYSTEM

LFEDA was constructed by the Chinese Academy of Meteorological Sciences in 2014 at the Guangdong

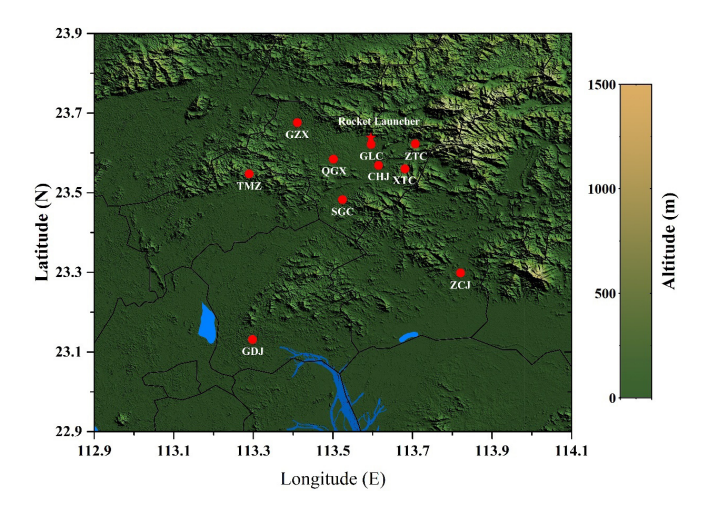


Fig. 1. Current geographical layout of the LFEDA sensors in the Guangzhou area after 2017. The colors represent the altitude (units: m), and the stations are represented by circles. Experiments with artificially triggered lightning were conducted at the position marked by the red star.

Comprehensive Observation Experiment on Lightning Discharge (GCOELD) in Conghua District, Guangzhou, and a preliminary observation test was carried out that same year. A detection network composed of nine substations was initially formed in 2015 [1], [23], [26]. At present, in accordance with thunderstorm observation practice in recent years, station GDJ has been added to the original nine stations, and the original station at site SLC has been relocated to ZTC, forming a synchronous lightning field detection system consisting of ten stations (Fig. 1). For the eight stations other than GDJ and ZCJ, the baseline lengths are 6-42 km, while GDJ and ZCJ are positioned to enhance the system's ability to detect and locate lightning during large-scale thunderstorms. ZCJ is located relatively far from the other eight stations, at baselines of 30-61 km, and similarly, the baselines of station GDJ are 45-70 km.

The equipment used to probe the electric field changes at each LFEDA substation is a traditional fast antenna [22]. The signal detection band of LFEDA's fast antennas is 160 Hz-600 kHz, and the time constant is 1 ms. The wide working frequency band ensures that the signals collected by the system capture rich characteristics of the electric field changes during the lightning process in both the time and frequency domains. This not only enables the identification and analysis of the physical processes of lightning based on the waveform characteristics in this VLF band but also ensures that the system can detect a sufficiently large number of electric field pulse signals. Data acquisition is based on floating level triggering to eliminate the impact of LF variations on data acquisition; 1-ms segmented synchronous recording, acquisition, and storage are used to realize the no-dead-time acquisition of the waveforms showing the changes in the lightning electric field, and the pretrigger time is set to 200 μ s. The sampling rate used for the acquisition of the waveform data is 10 MHz, and the resolution is 12 bits. Synchronization among the different substations is realized by means of a GPS clock with a time accuracy of 50 ns.

LFEDA mainly focuses on the fast electric field change pulse signals generated during the lightning discharge process. For positioning, three steps are needed: waveform matching, pulse searching, and pulse matching. After pulse matching, the peak times of the pulse discharge events are obtained, and the time differences between the peaks of the same pulse at different stations are calculated. The 3-D position of each pulse discharge event is determined using a nonlinear least-squares fitting algorithm [23], as is common practice in current lightning location research. Fan et al. [1] introduced EMD [24], [27]–[29] into the location algorithm for the first time on the basis of the nonlinear and discontinuous characteristics of the LF/VLF electric field change signals generated by lightning and the ultrawideband characteristics of the electric field detection equipment. The intrinsic mode functions (IMFs) of the electric field waveforms are obtained through EMD, and the features of each IMF component are analyzed using the fast Fourier transform (FFT) to realize low-frequency filtering and high-frequency noise reduction of the waveforms. Using the second cross-correlation method and the Hilbert transform with a reduced time window scale to fully extract the pulse signals from the fast lightning electric field waveforms and reduce the time errors of the peak pulse values, a TOA lightning location algorithm has been developed based on the precise analysis and processing of the electric field signals.

III. ALGORITHM INTRODUCTION

The LF/VLF electromagnetic field signal generated by lightning is a typical nonlinear and nonstationary signal. The 160 Hz-600-kHz frequency band of the LFEDA system can capture rich characteristics of the electric field changes that occur during the lightning process in both the time and frequency domains. This not only enables the identification and analysis of the physical processes of lightning based on the wave characteristics in this VLF band but also ensures that the system can detect rich electric field pulse signals. However, the large relative bandwidth also means that the detected waveform components of the lightning electric field are very complex, which leads to two problems. On one hand, the VLF electric field components and background noise make the matching and recognition of lightning pulse signals more difficult. On the other hand, the relatively high-frequency signal components (including the high-frequency part of the Gaussian white noise and background noise signals from other sources) will shift the peak values of the VLF lightning pulse signals, resulting in large errors when the TOA location method is used.

Fan et al. [1] introduced the EMD algorithm into the analysis of the LF/VLF lightning electric field signals for signal optimization. EMD was first proposed by Huang et al. [24] as a nonlinear multiresolution adaptive decomposition method, different from the traditional Fourier transform, wavelet transform, and other methods. It serves as an alternative signal processing technique based on an empirical and algorithm-defined method. EMD can adaptively decompose a complex signal into a set of complete, almost orthogonal components,

that is, IMFs, without requiring any preliminary understanding of the nature and quantity of the IMF components in the data. EMD can be used to decompose a signal without specifying the basis functions in advance, and the degree of decomposition is adaptively determined in accordance with the nature of the signal to be decomposed; this is the main advantage of EMD compared with the widely used wavelet-based technique. Because of its excellent performance, EMD has been widely used in many disciplines [29].

The introduction of the EMD algorithm significantly improves the identifiability of the pulse signals of lightning electric fields and somewhat reduces the error on these lightning signals, thus making the acquired pulse information and positioning results richer and more accurate, and the findings objectively show that EMD offers unique advantages in the analysis of lightning electromagnetic field signals [1]. However, with further research, it has been found that the EMD algorithm is also subjected to inherent mode mixing and endpoint effects, which lead to problems in the analysis of the LF/VLF electric field change signals. Mode mixing is defined as a phenomenon in which either a single IMF includes oscillations of significantly different scales or signals of similar scales are decomposed into different IMF components, and it is caused by signal discontinuity [30]. Mode mixing leads to a loss of pulse power and the undesired retention of some noise signals, while the endpoint effect causes distortion of the reconstructed signal, which leads to inaccurate electric field pulse recognition and peak time extraction. For lightning location based on the detection of LF/VLF electromagnetic fields, the accuracy of electromagnetic pulse time extraction and the sufficiency of pulse recognition are the keys to improving the lightning location ability [1], [23].

To solve the problems above, this article introduces the ensemble EMD (EEMD) algorithm into the analysis of the LF lightning electromagnetic signals and proposes a corresponding filtering method (DBM_EEMD) based on the use of a double-sided bidirectional mirror (DBM) extension of the original signal to mitigate the endpoint effect. In this way, the accuracy of electric field pulse time extraction and the sufficiency of pulse recognition are improved to further enhance the lightning positioning performance of the LFEDA system.

A. Ensemble Empirical Mode Decomposition

To overcome the inherent mode mixing problem of the EMD algorithm [24], Wu and Huang [30] proposed the EEMD algorithm, which is a very effective noise-aided data analysis (NADA) method. In EEMD, white-noise signals $n_i(t)$ are added to the original signal x(t). Because the white-noise spectrum is evenly distributed, the white-noise signals will be automatically distributed to the appropriate reference scales. Moreover, because of its zero-mean characteristic, the white noise will cancel itself out after many rounds of averaging; hence, the result obtained by calculating the ensemble mean can be directly taken as the final result. The specific steps of the EEMD algorithm are as follows, and a flow chart of the algorithm is shown in Fig. 2.

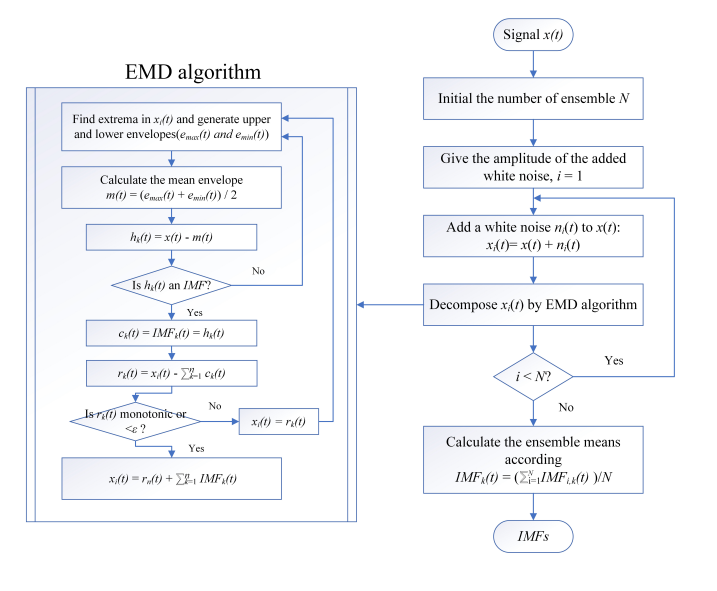


Fig. 2. Flowchart of the EEMD algorithm.

- 1) Initialize the number of ensemble members, N.
- Specify the amplitude of the added white noise and set
 i = 1
- 3) Add a numerically generated white-noise signal $n_i(t)$ to the original signal x(t) to generate the new signal $x_i(t)$

$$x_i(t) = x(t) + n_i(t) \tag{1}$$

where $n_i(t)$ denotes the *i*th white-noise series, with i = 1, 2, ..., N.

4) Use the original EMD algorithm to decompose $x_i(t)$ into IMFs

$$x_i(t) = \sum_{k=1}^{n} c_{i,k}(t) + r_{i,k}(t)$$
 (2)

where n is the number of IMFs, $r_{i,k}(t)$ are the final residues, and $c_{i,k}(t)$ are the IMFs themselves $(c_{i,1}(t), c_{i,2}(t), \ldots, c_{i,n}(t))$, which include different frequency characteristics, from high to low bands, extracted from $x_i(t)$.

 Repeat steps (3) and (4) N times with a different white-noise signal each time to obtain an ensemble of IMFs

$$[\{c_{1,k}(t)\}, \{c_{2,k}(t)\}, \dots, \{c_{N,k}(t)\}]$$
 (3)

where k = 1, 2, ..., n.

6) Calculate the ensemble means of the decomposed IMFs using the following function:

$$IMF_k(t) = \frac{1}{N} \sum_{i=1}^{N} c_{i,k}(t)$$
 (4)

where $i=1,2,\ldots,N$ and $k=1,2,\ldots,n$. Then, $\mathrm{IMF}_k(t)$ is the kth IMF component obtained through EEMD.

Fig. 3 shows a 1-ms lightning electric field waveform and the corresponding decomposition results obtained through EMD and EEMD. There are significant differences between

the decomposition results of the different algorithms for the same electric field waveform. These differences in the decomposition results lead to different lightning location capabilities based on multistation electric field measurements.

B. Mode Mixing in EMD

To illustrate the differences between the decomposition results shown in Fig. 3 and the problems that arise in the analysis of the LF/VLF lightning electric field signals for lightning location, a simulated signal $s(t) = 25 \times \sin(100000 \times pi \times t) + 20 \times \sin(250000 \times pi \times t) + 50$ is used to simulate the pulse signal characteristics of an electric field generated by lightning, and the simulated detected signal s'(t) is generated by superposing Gaussian white noise with a mean value of 0 onto s(t). A corresponding noisy simulated signal collected over a duration of 1 ms at the 10-MHz sampling rate of the LFEDA detection system is shown in Fig. 4. Due to the presence of noise, the peak positions of the pulse signals are shifted; however, the capability of TOA-based lightning pulse location relies on accurate multistation measurements of lightning electric field pulses [1].

The results of decomposing s'(t) through EMD and EEMD are shown in Fig. 5. By comparing the IMF components of the same order in panels a and b of Fig. 5, we can see obvious differences in the signal decomposition results, especially for IMF 4 and IMF 7. The frequency and amplitude characteristics of these two IMF components in Fig. 5(a) are messy, and it is difficult to distinguish the main signal characteristics captured by each component, while the frequency and amplitude characteristics of all the IMF components in Fig. 5(b) are clear.

In the Hilbert-Huang transform (HHT), the Hilbert transform is applied to the IMF components obtained through EMD, and the FFT is used to obtain the single-side spectrum characteristics of each IMF component [29]. The HHT results for IMFs 4–6, which show the most significant differences in Fig. 5, and for the original signal s(t) are shown in Fig. 6. The simulated signal s(t) is composed of two main signals at frequencies of 50 and 125 kHz. It can be seen from Fig. 6(a) that with EMD, the characteristics of the 50-kHz signal are almost equally decomposed into IMF 5 and IMF 6. The signal at 125 kHz is also decomposed into two IMF components (IMF 4 and IMF 5), and wideband noise is present in all three of these IMF components. Thus, mode mixing is observed: a single IMF (IMF 5) contains significant oscillations at different scales, and signals of similar scales are decomposed into different IMF components. In contrast, EEMD, in which noise signals are introduced for auxiliary analysis, can cleanly decompose the main characteristics of the simulated signal into different IMF components, and it can be seen from Fig. 6(b) that the noise signal components are well-suppressed in each resulting IMF component.

The so-called mode mixing effect will cause several problems in the lightning electric field signal analysis. On one hand, noise cannot be fully filtered out, so the peak values of the electric field pulses will still have some errors. On the other hand, part of a single pulse feature decomposed into multiple IMF components may be filtered out by a bandpass filter,

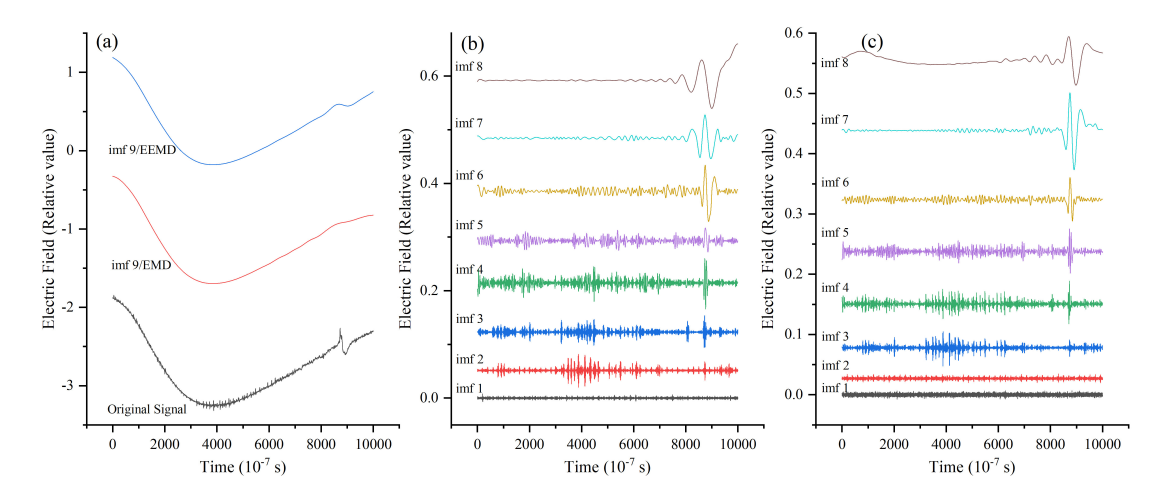


Fig. 3. Decomposition results for a 1-ms electric field waveform. (a) Original electric field waveform and the ninth IMF components obtained through EMD and EEMD. (b) First-eighth IMF components obtained through EMD. (c) First-eighth IMF components obtained through EEMD.

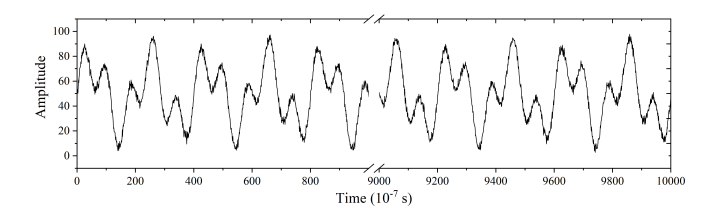


Fig. 4. Simulated signal s'(t) with superposed Gaussian white noise.

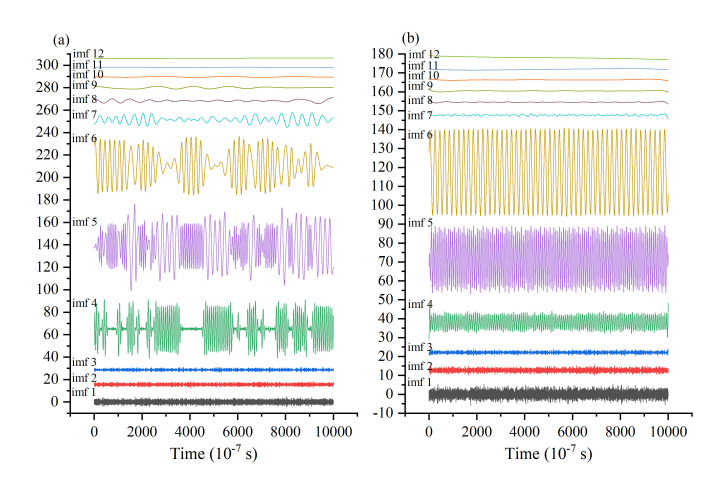


Fig. 5. Results of decomposing noise-added simulated signals through EMD and EEMD. (a) Results of EMD. (b) Results of EEMD.

resulting in large signal energy loss. Weak signals decomposed into high-frequency IMF components may even be filtered out entirely. All these problems affect the sufficiency and accuracy of pulse signal detection in low-frequency electric field pulse location and thus affect the convergence and continuity of lightning channel mapping.

C. Endpoint Effect and Double-Sided Bidirectional Mirror Extension

Due to the lack of extreme points at the end of the signal, using a spline difference method to fit the upper and lower

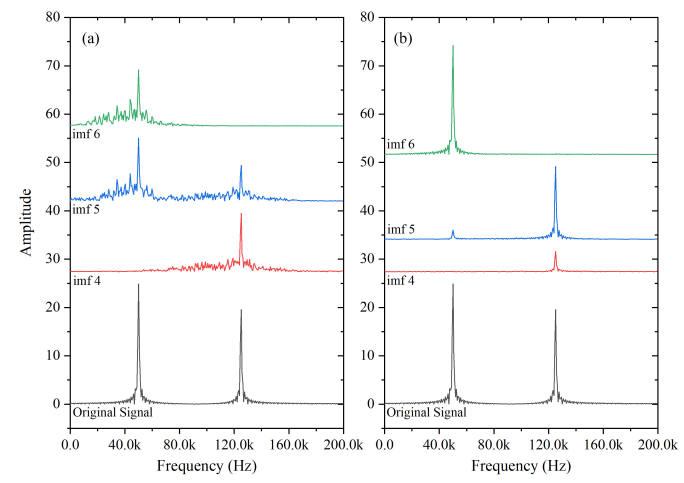


Fig. 6. Spectra of IMFs 4–6 in Fig. 5. (a) As obtained through EMD. (b) As obtained through EEMD.

envelopes will lead to a large signal error at the boundary. This error will further worsen the decomposition result for the middle part of the signal obtained in the EMD filtering process, resulting in the pollution of the whole signal sequence; this phenomenon is called the endpoint effect of the EMD algorithm [29]. As shown in Fig. 7, the endpoint effect will lead to signal distortion and a shift in pulse position. When LF/VLF lightning electric field measurements are used for positioning, this effect will also cause problems such as poor signal correlation between stations and inaccurate pulse time extraction.

There are many ways to suppress the endpoint effect. However, in practical engineering applications, the mirror extension method [28], which can effectively suppress the endpoint effect to a certain extent, has been one of the more widely used methods for this purpose because of its simplicity and versatility. In the actual analysis of the lightning electric field signals, it has been found that the frequency spectra of the ultrawideband and LF electric field signals collected by

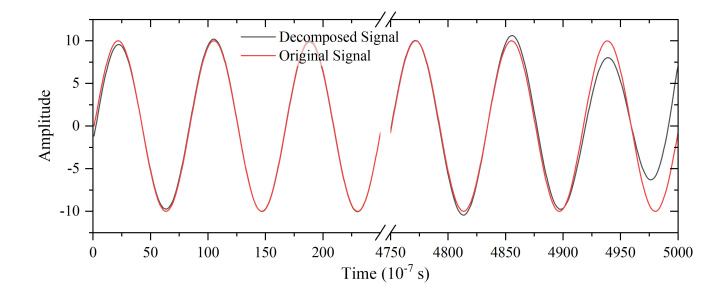


Fig. 7. Schematic of the endpoint effect.

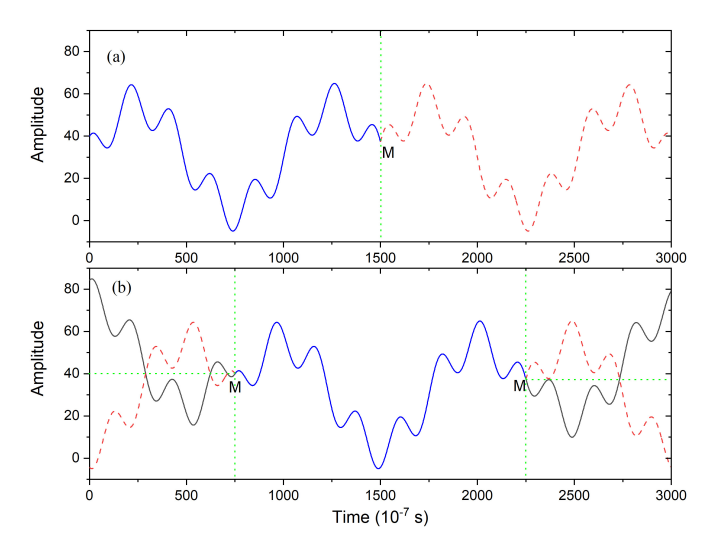


Fig. 8. Diagrams of mirror extension. (a) General mirror extension. (b) DBM extension. The blue solid line represents the original signal, the red dotted lines represent the left and right mirror-extended signals, the black solid lines represent the signals obtained through the mirror reversal of the mirror-extended signals in the vertical direction, and the green dotted lines indicate the mirror points.

LFEDA are very complex, and the nonlinear and discontinuous characteristics of these signals are obvious. In the development of algorithms for batch data processing, analysis, matching, and positioning, the universality of these algorithms is an important concern. Therefore, we have attempted to use mirror extension for endpoint effect suppression.

However, due to the complexity of the LF/VLF lightning electric field signals and the stringent requirements for pulse information extraction in the lightning location process, simple mirror extension has certain limitations for positioning based on such signals. This is because, as long as there is a signal at the endpoint, whether it is of relatively high frequency or relatively low frequency, the mirror-extended signal and the original signal together form a mutated signal that is not differentiable at the mirror point [point M in Fig. 8(a)]. In the actual signal decomposition process, this nondifferentiable point will have a significant impact on the decomposition results. Fig. 9(a) shows the results of applying EEMD after the left-right symmetrical image processing of the simulated signal s'(t). It can be seen that the various IMF components generally exhibit significant vibration and distortion at M. This problem is especially serious for positioning using lightning

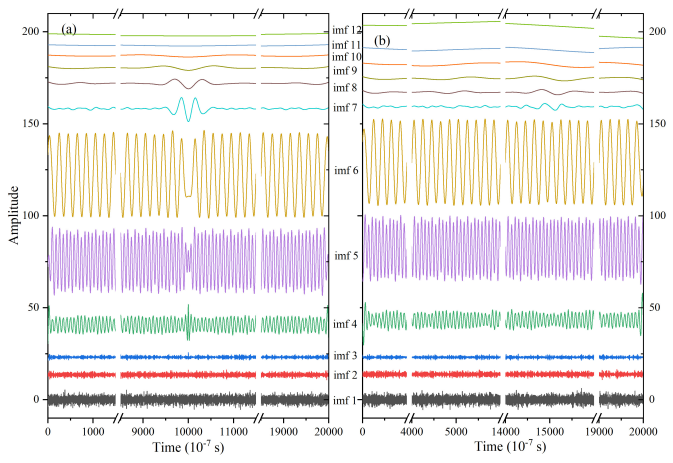


Fig. 9. Comparison of the decomposition results for the mirror-extended and DBM-extended signals. (a) Decomposition results for a mirror-extended signal with the mirror position at 10 000. (b) Decomposition results for a DBM-extended signal (DBM_EEMD) with the horizontal mirror positions at 5000 and 15 000.

electric fields: when an electric field signal is passed through a bandpass filter [1], the reconstructed signal suffers severe distortion and a loss of signal energy, which will also lead to poor correlations and large pulse time errors in multistation signal matching.

To solve the above problems, this article proposes the DBM extension method. As shown in Fig. 8(b), in contrast to the general mirror extension [shown in Fig. 8(a)], the DBM extension method involves extending the original signal with two image signals [shown as the red dotted lines in Fig. 8(b)], each with half the length of the original signal and extending outward from the left and right ends of the original signal, and then reversing these two image signals in the vertical direction to obtain the vertical image of each horizontal image signal [shown as the black solid lines in Fig. 8(b)]. Hence, this method is both double-sided (left and right) and bidirectional (horizontal and vertical). The extended image signals [black solid lines in Fig. 8(b)] are combined with the original signal to form the signal to be decomposed. As seen from Fig. 8(b), the DBM extension effectively solves the problem of signal mutation at the end of the original signal caused by mirror extension (as shown at M).

The IMF components obtained by applying EEMD to the extended signal after DBM extension of the simulated signal s'(t) are shown in Fig. 9(b). By comparison with the EEMD results for the general extended image signal shown in Fig. 9(a), it can be seen that the severe distortion of the IMFs at the discontinuity point (M) of the signal constructed through mirror extension is significantly suppressed in the IMFs obtained from the DBM-extended signal.

D. Bandpass Filtering

Based on the ability of EMD to decompose discontinuous and nonstationary signals into finite IMF components, Fan *et al.* [1] introduced the EMD algorithm into the analysis of the LF/VLF lightning electric field signals and constructed a bandpass filter suitable for lightning location.

Specifically, only the IMF components in the frequency range of 3–300 kHz obtained by decomposing the electric field signal detected by LFEDA are recombined. On one hand, this filtering process significantly suppresses the interference from the VLF components of the electric field signals in multistation waveform matching, thus improving the accuracy and sufficiency of pulse recognition. On the other hand, the interference of high-frequency noise in the pulse peak times is reduced. Thus, the accuracy of the LFEDA system in locating the LF/VLF electric field pulse signals generated by lightning is significantly improved, giving the system the ability to locate lightning channels to a certain extent.

However, as described in the above analysis, EMD is inherently subjected to mode mixing and endpoint effects, which greatly affect the accuracy of decomposition and feature extraction for electric field pulse signals. The establishment of the 3–300-kHz bandpass filter is essentially a compromise scheme that considers LF component suppression, noise level reduction, and signal energy loss. In the absence of a different signal processing approach, the EMD algorithm and the 3–300-kHz bandpass filtering scheme significantly improve the lightning location capabilities of LFEDA. However, based on the above analysis of the existing problems with EMD, it seems preferable to seek alternative solutions.

EEMD, in which noise signals are introduced for auxiliary analysis, can effectively suppress the mode mixing effect, whereas mirror extension of the signal can effectively suppress the endpoint effect. To mitigate the problem of signal distortion caused by the discontinuity at the end of the original signal in the general mirror extension method, this article instead proposes the novel DBM extension method. The EEMD and DBM extension methods can together be applied to improve the analysis of the lightning electric field signals detected by LFEDA. Based on an analysis of the characteristics of these electric field signals and empirical tests of the effectiveness of signal processing in actual lightning location research, we set the bandpass filter parameters to select the frequency range between 25 and 500 kHz.

To illustrate the performance differences in different algorithms, the noisy signal s'(t) introduced above is used again here for further simulation analysis. Fig. 10 shows a local comparison of the two ends of the reconstructed signal obtained after passing the noisy signal through the 25–500-kHz bandpass filter. It can be intuitively seen that there are several differences between the reconstructed signal and the original simulated signal. To evaluate the performance differences among the considered filtering methods, based on the actual needs of lightning positioning research, two indexes are used to quantitatively evaluate the performance of each filter: the noise reduction ability of the filter and the root-mean-square (rms) error between the filtered signal and the original signal.

Fig. 11 compares the distribution of the offset errors of the peak positions in the reconstructed signal after the 25–500-kHz bandpass filter (red columns) with the distribution of the pulse peak offsets of the noisy signal (black columns). It can be seen from Fig. 11(a) that the bandpass filter constructed through EMD has a certain noise reduction ability, but the effect is not significant; in fact, it is worse than that of the 3–300-kHz

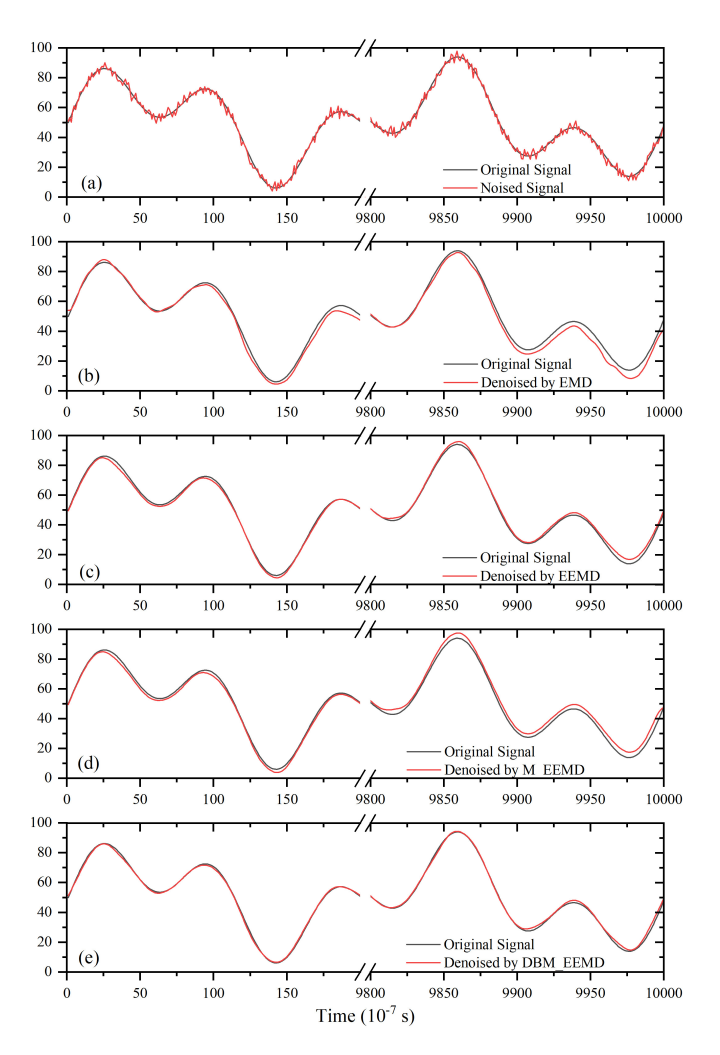


Fig. 10. Comparisons between the original and noise-reduced signals obtained after applying bandpass filters constructed using different EMD algorithms. (a) Original signal with and without noise. (b)–(e) Comparisons of the original simulated signal with the results of EMD, EEMD, M_EEMD, and DBM_EEMD filtering, respectively.

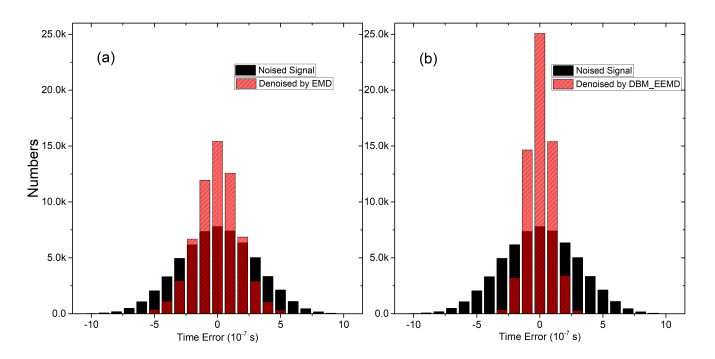


Fig. 11. Distributions of the peak position deviations between the noisy signal and the original signal (black columns) and between the noise-reduced signal and the original signal (red columns). These statistical results were obtained from 500 simulation experiments based on the simulated signal shown in Fig. 4. (a) Simulated results of high-frequency filtering through EMD. (b) Simulated results of high-frequency filtering through DBM_EEMD.

filter adopted by Fan *et al.* [1]. In contrast, the bandpass filter constructed through DBM_EEMD exerts a significant effect in suppressing the noise-induced peak time error. After filtering, the peak time error for nearly 85% of the pulses is less than

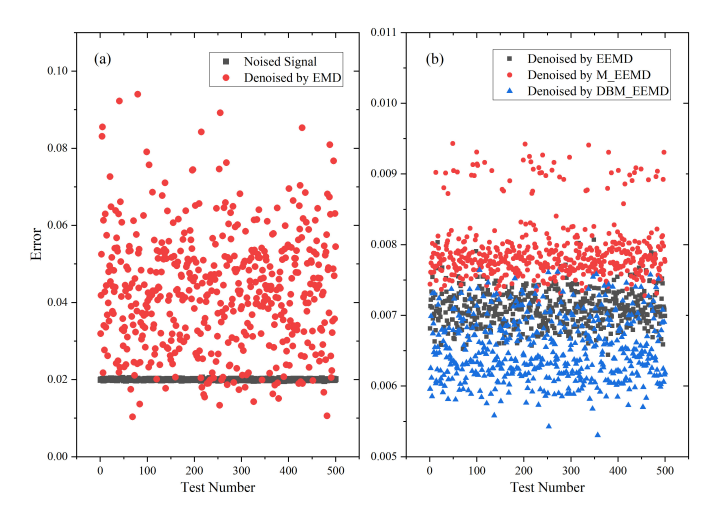


Fig. 12. Simulation of the errors between the reconstructed signals obtained after bandpass filtering and the original signal without noise. These results were obtained through 500 simulation experiments based on the simulated signal shown in Fig. 4. (a) Comparison of the RMS errors of noisy signals and EMD-denoised signals. (b) Comparison of the rms errors of EEMD-, M_EEMD-, and DBM_EEMD-denoised signals.

100 ns (the time resolution of LFEDA at its 10-MHz sampling rate is 100 ns).

The noise reduction ability of a signal processing algorithm is the most important performance index when using the LF/VLF lightning electric field pulse signals for lightning location. In addition, when the EMD algorithm is used to filter an electric field waveform to extract the characteristic pulse signal, the loss of signal amplitude is also an important performance index. This is because the accurate extraction of pulse feature signals is helpful for improving the accuracy of multistation waveform and pulse signal matching using the cross-correlation method [1], and the signal fidelity is particularly important for the effective detection of electric field pulses. Here, the RMS error of a signal before and after bandpass filtering is defined as follows:

$$Error = \frac{\operatorname{sqrt}\left(\sum_{i=1}^{N} (s(t) - s'_{D}(t))^{2}\right)}{N}$$
 (5)

where s(t) is the original signal without noise, $s_D'(t)$ is the noise-reduced signal after bandpass filtering, and N is the signal length. In particular, the electric field waveforms collected by LFEDA at a sampling rate of 10 MHz consist of 10 000 sampling points per 1-ms segment.

Fig. 12 plots the RMS signal errors calculated from 500 simulation experiments. The following conclusions can be drawn from this figure. When a signal is decomposed through EMD, filtered with a bandpass filter and then recombined, although the time errors of the pulse peaks can be reduced to a certain extent [as shown in Fig. 11(a)], severe pulse signal distortion occurs due to mode mixing and the endpoint effect [as shown in Fig. 12(a)]; moreover, this signal distortion is extremely unstable across many different simulation experiments. In contrast, after the bandpass filter constructed based on the EEMD algorithm, the RMS signal error is generally reduced [as shown in Fig. 12(b)]. However, because mirror extension creates a discontinuity at the end of the signal,

the IMF components will be distorted at the end, which may, in turn, cause distortion of the reconstructed signal. From the comparison in Fig. 12(b), it can be seen that because of this problem, the error of the reconstructed signal obtained by passing a noisy signal through the M_EEMD filter is larger than that achieved with the EEMD method. In contrast, when a noisy signal is passed through the DBM_EEMD filter, the error of the reconstructed signal is even lower than that achieved with EEMD, and the reconstructed signal quality is significantly better than that achieved through M_EEMD.

IV. POSITIONING PERFORMANCE

In this article, to overcome the problems with the EMD algorithm introduced into the lightning electric field signal analysis by Fan et al. [1], the EEMD algorithm is instead applied to this analysis problem because of the high demand for signal accuracy in lightning location. To further mitigate the distortion caused by mirror extension near the end of a signal, the DBM extension method is proposed, which significantly reduces the distortion of a lightning electric field signal passed through a bandpass filter. Based on an empirical test of the actual multistation positioning effect, a bandpass filter of 25–500 kHz is established. The introduction of these improved signal processing methods further enhances the lightning location capabilities of LFEDA. On one hand, we have performed repositioning analyses for the lightning cases introduced in Fan et al. [1] and found that the positioning effect is further improved; on the other hand, the introduction of DBM EEMD gives the LFEDA system the ability to locate channels of artificially triggered lightning, which could not be done in the past because the corresponding electric field signals are usually weak.

A. Hybrid Flash

Fig. 13 shows the repositioning results for a hybrid flash introduced in Fan *et al.* [1]. Other than the new filter parameters set using DBM_EEMD, the positioning parameters are consistent with those used in Fan *et al.* [1]. Compared with the EMD algorithm, the DBM_EEMD algorithm can obtain better positioning results; the main improvements are reflected in the matching accuracy for the electric field signals detected by remote stations and the detection ability and accuracy for weak pulse signals.

First, the improvement in the positioning ability is reflected in the improved matching accuracy for the electric field signals detected by remote stations. From the 3-D image obtained through positioning analysis, it can be seen that the lightning channel starts at 7.3 km above station XTC and extends over a wide range to the southwest and northeast of the station network, with channel branches extending to the northwest. Due to a power supply interruption affecting the equipment at station GZX in the northwest part of the station network during the thunderstorm, most stations in the station network were far away from the northwestern lightning channel branches; consequently, only a small amount of the electric field waveform generated during the lightning process was detected, and the signals are weak. Therefore, the insufficient processing

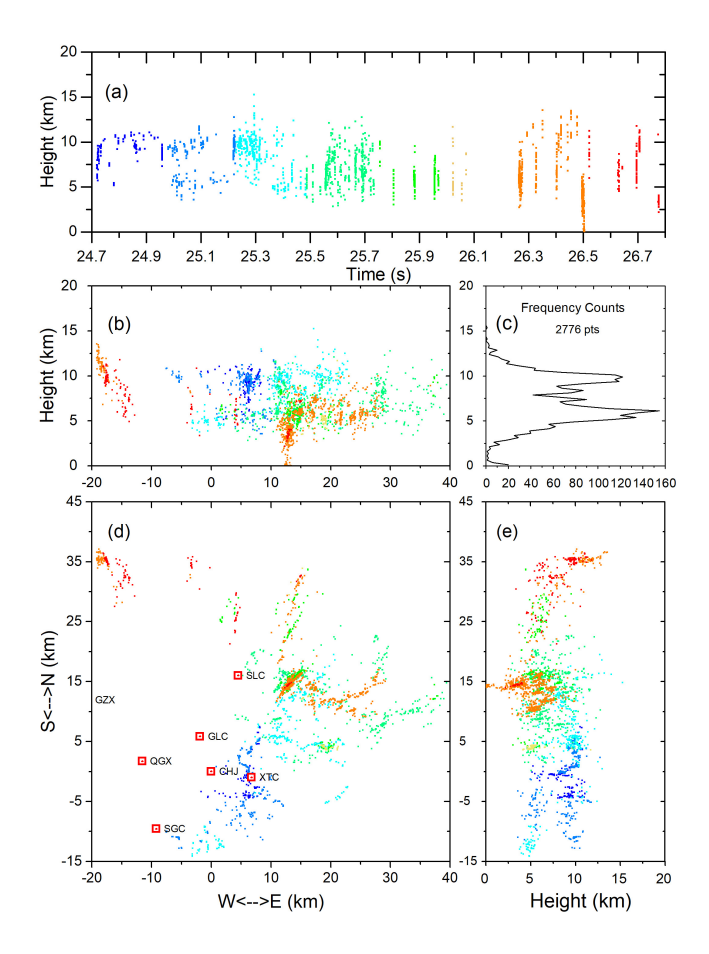


Fig. 13. Location results for negative ground flash CG201508151626 obtained using the DBM_EEMD method. (a) Height-time plot. (b) North-South vertical projection. (c) Height distribution of a number of radiation events. (d) Plane view. (e) East-West vertical projection of the lightning radiation sources.

ability of the EMD algorithm for these weak partial signals leads to relative divergence of the channel description obtained through the positioning algorithm. The main reason is that the error of EMD filtering for weak signals is large, in turn resulting in large errors for multistation matching and pulse peak time extraction. In contrast, the error for the electric field waveforms processed through DBM_EEMD is significantly reduced, thus also improving the errors for multistation matching and pulse peak time extraction. As seen from the repeated verification of the matching electric field waveforms and the overlapping channel features correspondingly developed in the positioning results, the reliability of the positioning results for signals detected far from the northwest part of the station network is significantly improved.

The improvement in the positioning ability is further manifested in the significant improvement in the positioning ability for the leader-return stroke channel. The channel breakdown process before the return stroke is usually characterized by a relatively high-frequency and weak signal. When such a signal is detected at a far distance in a long-baseline network, the acquired signal is usually severely attenuated. In the processes of waveform matching, Hilbert transformation, and pulse peak seeking, such weak high-frequency signals and return stroke electric field waveform signals are used together.

Problems of incorrect matching can easily arise, and pulse information cannot be effectively extracted. Even the small number of successfully matched weak pulse signals will be subject to large errors due to the low signal-to-noise ratio. However, when DBM_EEMD is introduced into the positioning process, on one hand, it can effectively reduce the signal energy loss caused by EMD filtering, thus enhancing the signal detection ability of the positioning algorithm under the condition of constant parameters; on the other hand, it can further improve the signal noise reduction ability, thus ensuring that the peak times extracted from the detected signals by the positioning algorithm are more accurate. Consequently, more pulse location points can meet the screening conditions.

The improvement in the positioning ability is also shown by the fact that the number of effective positioning points is significantly increased when other parameters remain unchanged. In [1], a total of 2296 pulse positioning points were obtained for CG201508151626. In this study, 2776 pulse positioning points were obtained with DBM_EEMD, with all other parameters remaining unchanged. The additional positioning points are mainly concentrated in the upper positive charge region [Fig. 13(c)], indicating that the electric field signals generated by the discharge process in this region are relatively weak in the LF/VLF band. Early scholars [31]-[36] analyzed the charge structure of thunderclouds by considering the layered characteristics of the location results for lightning radiation sources in the VHF band and concluded that the negative leader propagates in the positive charge region, which is characterized by a dense distribution of radiation sources, whereas the positive leader propagates in the negative charge region; however, because the radiation signal of the positive leader could not be easily detected, fewer location results were obtained for the negative charge region. Thus, it can be seen that the electromagnetic signal produced during the lightning discharge process has significantly different radiation characteristics in different frequency bands. These differences need to be studied and discussed on the basis of synchronous observations from detection equipment operating in different frequency bands; for this reason, it is necessary to further develop the capabilities of the LF/VLF lightning detection systems, even though many VHF lightning positioning systems are already capable of obtaining fine lightning positioning results.

Moreover, the new location results reported here show better convergence and continuity in local details, as can be seen directly from a simple comparison of the results. By analyzing the electric field waveform data group by group, it is found that the local discontinuities of the lightning channel observed in the positioning results may be caused by the measures adopted in LFEDA to suppress a large number of false triggers caused by environmental noise; the selected trigger threshold is high, thus preventing the collection of many electric field signals from pulse discharges.

B. Artificially Triggered Lightning Event

The purpose of LFEDA is to study the charge structure of thunderclouds and the physical processes of natural lightning

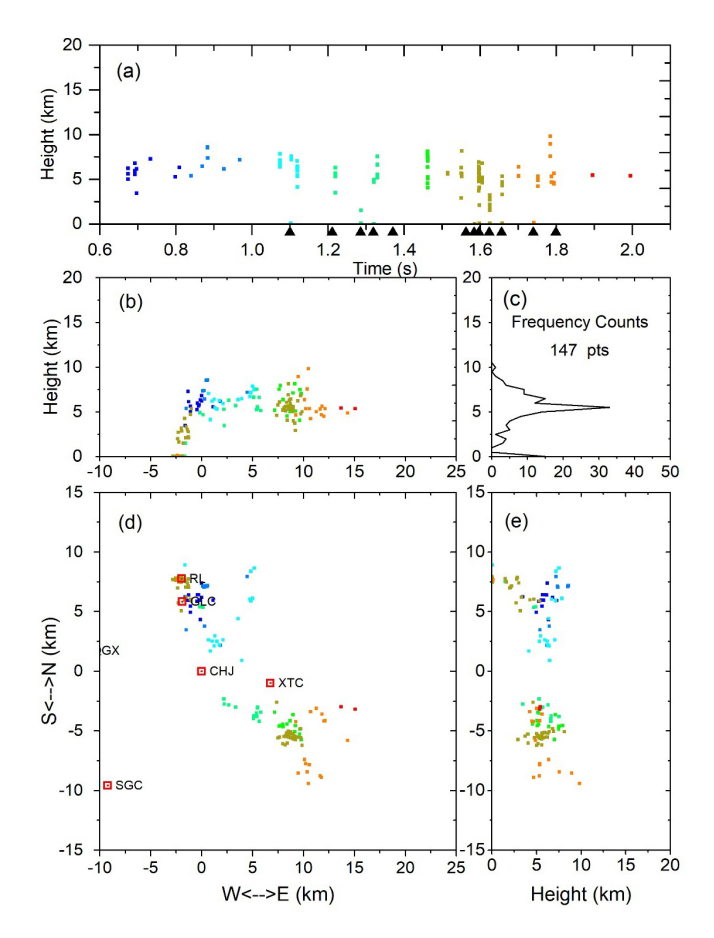


Fig. 14. Location results for artificially triggered lightning event CG201508141526 obtained using the EMD algorithm. (a) Height-time plot. (b) North–South vertical projection. (c) Height distribution of a number of radiation events. (d) Plane view. (e) East–West vertical projection of the lightning radiation sources. The black arrows indicate the times and locations of return strokes.

discharges and artificially triggered lightning [9], [37], [38]. The layout of the station network was designed by referring to the layout characteristics of several similar station networks. Generally, the baseline lengths are relatively long. Given the current state of development of lightning location capabilities, such a station network layout, combined with traditional electric field detection equipment and the segmented acquisition method, is favorable for the monitoring of lightning activity during large-scale thunderstorms, and under certain conditions, good positioning results can be obtained for some natural lightning discharge processes. However, for artificially triggered lightning, although its physical processes are no different from those of natural cloud-to-ground (CG) lightning in some respects, triggered lightning does not involve the stepped leader and first return stroke of natural CG lightning. The discharge pulses that occur in the process of a dart or stepped-dart leader prior to the subsequent return stroke in triggered lightning are relatively weak, and because of the severe attenuation that occurs in long-distance signal transmission, a long-baseline LF/VLF electric field detection system usually cannot synchronize enough discharge pulses to realize the positioning of the corresponding development channel. At present, there have been no reports of a long-baseline positioning system operating in a similar frequency band that

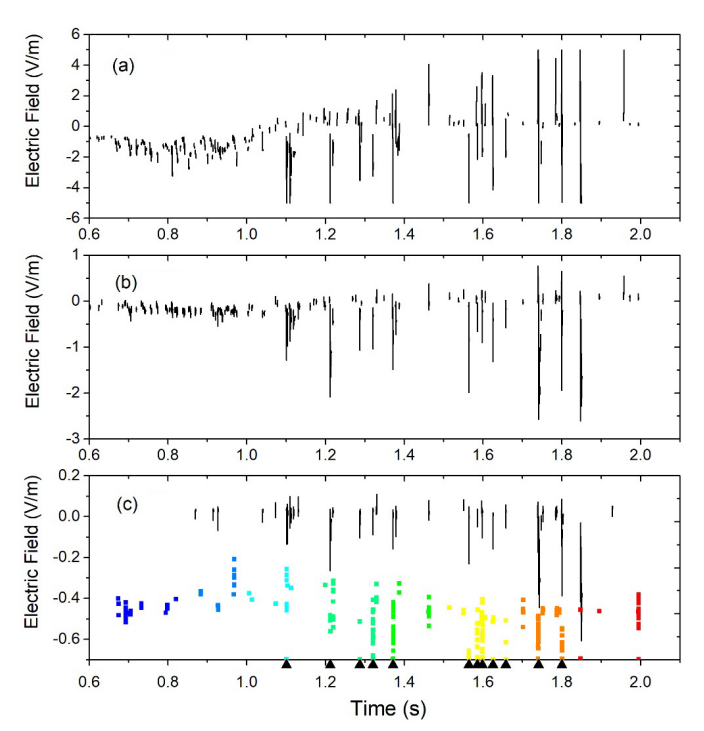


Fig. 15. Segmented electric field waveforms of the artificially triggered lightning event detected by LFEDA stations at different distances. (a) Detected electric field at station CHJ. (b) Detected electric field at station SGC. (c) Detected electric field at station ZCJ superimposed with the location results from the time-height map obtained with the DBM_EEMD algorithm [the same as Fig. 16(a)]. The black arrows indicate the times of return strokes.

is able to obtain more abundant positioning information in addition to the return stroke position for artificially triggered lightning.

By strengthening the performance of signal analysis techniques, the waveform matching, pulse extraction, and accurate positioning capabilities of LFEDA for weak pulse signals have been continuously improved. Fig. 14 shows the location results obtained using EMD signal processing for an artificially triggered lightning case (CG201508141526) with 12 measured return stroke currents [1]. For this triggered lightning case, data from only seven stations (GLC, CHJ, SGC, SLC, TMZ, XTC, and ZCJ) are available, and station GLC is located only 1.8 km away from the rocket launcher (the red star in Fig. 1). Under such short-range conditions for electric field detection, the electrostatic field component (manifesting as an ultralow-frequency signal) in the lightning electric field signal is too strong and can easily reach saturation. Even at station CHJ, which is 8 km away from the rocket launcher, the electric field pulses for seven return strokes also reach saturation. In contrast, under far-field detection conditions, the signal is greatly attenuated; consequently, at station ZCJ, only the electric field waveforms of return strokes and a few discharge pulses in the cloud can be detected [as shown in Fig. 15(c)]. Therefore, even with the greatly improved positioning capability achieved by processing the LFEDA signals through EMD, only 150 positioning points can be obtained, and the positions of four return strokes cannot be accurately located. Although the locations of a few pulses in the leader-stroke channel can be determined, they are relatively

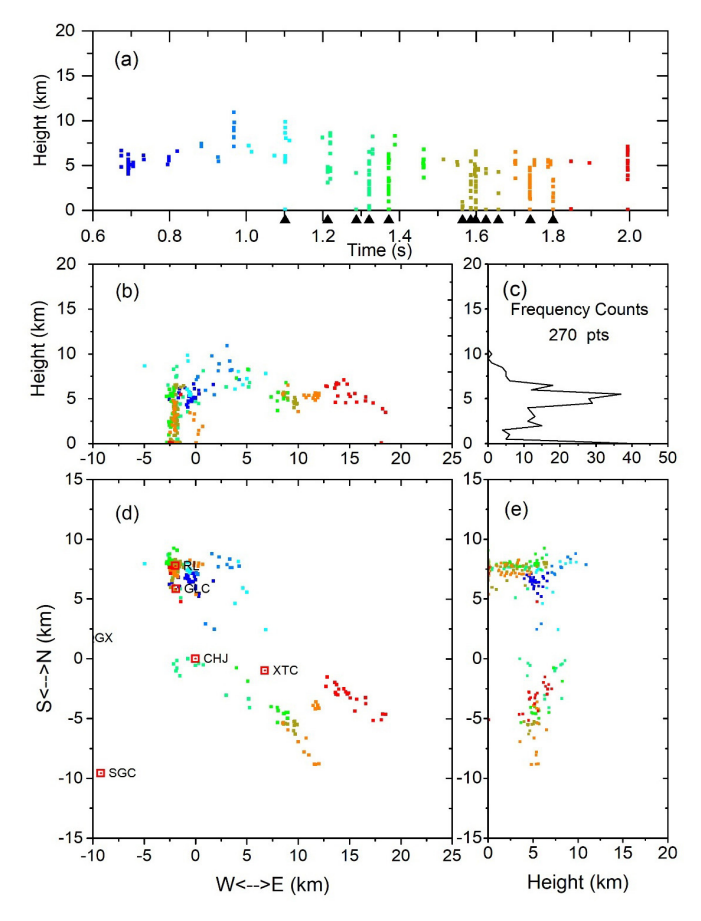


Fig. 16. Location results for artificially triggered lightning event CG201508141526 obtained using the DBM_EEMD algorithm. (a) Height-time plot. (b) North–South vertical projection. (c) Height distribution of a number of radiation events. (d) Plane view. (e) East–West vertical projection of the lightning radiation sources. The black arrows indicate the times of return strokes.

divergent and far from enabling the successful reconstruction of the stroke channel.

Fig. 16 shows a 3-D image of CG201508141526 obtained through DBM_EEMD under constant pulse extraction parameters. Compared with the positioning results in Fig. 14, despite the extremely complex signal characteristics and the fact that detected signals are available from only seven stations, the positioning results for the triggered lightning channel are obtained that provide not only the positions of 11 return strokes but also the position information for the discharge pulses of multiple subsequent return strokes in the stepped-dart leader process. Because the electric field pulses are too weak and the signal-to-noise ratio is too low during the leader process, the leader-stroke channel obtained through the positioning algorithm is relatively thick; however, these pulse positioning points still clearly provide a relatively complete description of the channel development characteristics. Thus, the positioning ability of the LFEDA system has been further improved by adopting the DBM_EEMD algorithm.

V. CONCLUSION AND DISCUSSION

From the above analysis, we can see that DBM_EEMD achieves a better noise reduction ability for the LF/VLF electric field signals and stronger fidelity for filtered signals

than the EMD algorithm does, thus further improving the ability of the location algorithm to detect pulse signals in the LF/VLF electric field waveforms and the accuracy of pulse time extraction. Thus, the accuracy of the location results is improved in turn, especially for the detection and location of a large number of weak pulse signals.

The original intent when building the LFEDA system was to study the physical processes of lightning and thunderstorm electricity and to use the return stroke pulses of triggered lightning generated at the GCOELD to test its positioning ability. Shi et al. [23] adopted mainstream LF/VLF lightning positioning techniques to develop the initial positioning capabilities of LFEDA, which enabled LFEDA to locate the return stroke pulses of ground flashes and discharge pulses in some clouds. The work of Fan et al. [1] gave LFEDA the ability to describe lightning channels to a certain extent. However, due to the mode mixing and endpoint effects of the EMD algorithm, a bandpass filter of 3–300 kHz will inevitably cause undesirable electric field signal attenuation and impaired noise reduction capabilities, resulting in insufficient pulse signal extraction, inaccurate pulse peak time extraction, and even the complete loss of weak signals. Therefore, because the electric field signals generated by the cloud process for artificially triggered lightning are relatively weak and the signal attenuation for long-distance detection is severe, there have been no previous reports of successful channel location for artificially triggered lightning using a long-baseline detection system such as LFEDA. Based on an analysis of the characteristics of the signals detected by LFEDA, a 25-500-kHz bandpass filter has been constructed in this article based on the improved DBM_EEMD algorithm, which significantly reduces the error on the reconstructed waveform obtained after filtering an electric field signal and significantly improves the accuracy of the multistation cross-correlation matching of electric field waveforms, the sufficiency of electric field pulse extraction, and the accuracy of pulse peak time extraction. Thus, we have developed the ability to use the long-baseline LFEDA system to locate the channel developed during an artificially triggered lightning flash based on the corresponding weak detected signals.

The detection and accurate positioning of lightning are highly dependent on the performance of the detection equipment, the layout of the station network, and the efficacy of the signal processing and analysis methods. For an LF/VLF lightning detection system with a working frequency band below 1 MHz, because of the large relative bandwidth, the detected electromagnetic signals are usually complex, and such LF/VLF signals can easily suffer from interference and attenuation. Consequently, the development of fine positioning capabilities for lightning discharge processes using such systems is lagging behind that of high-frequency lightning positioning technology. However, with the rapid development of lightning detection, electronic information, and signal analysis technology, it is possible to further refine the available capabilities for LF/VLF lightning electromagnetic field detection and positioning.

As an example, consider LFEDA, which uses traditional fast antennas as its electric field measurement equipment,

operates at 160 Hz-600 kHz, and uses a long-baseline station network layout. For this system alone, the existing research offers many possible improvements in terms of electric field measurement and positioning. On one hand, the working frequency band of the fast antennas used in LFEDA is relatively low compared with the working frequencies of other electric field detection equipment of the same kind. Although this low-frequency band ensures the ability to measure electrostatic components during the lightning discharge process, the ability to detect the characteristics of the radiation pulses generated during this process, which provide the most critical information for positioning, is insufficient. On the other hand, the time constant of the design circuits for the fast antennas used in LFEDA is 1 ms. This time constant is a characteristic parameter designed to enable the detection of changes in the fast electric fields associated with lightning given the (relatively insufficient) software and hardware capabilities typical of equipment developed in the middle of last century, which has been used for a long time. At present, however, the ability of a 1-ms time constant to respond to the changing pulse signals of electric fields is inadequate. With the development of higher performance electronic components, it has become easier to obtain more abundant pulse characteristics while guaranteeing successful electric field measurements using a more reasonable time constant. In addition, the LFEDA system is based on the segmented acquisition of lightning electric field signals; specifically, the signals are separated into segments of 1 ms in length, thus somewhat limiting the ability to describe the detailed development of lightning channels. This is because, depending on the actual detection environment, a high trigger threshold is usually set to prevent the collector from being triggered too frequently, which often results in incomplete detection of the electric field information for an entire lightning discharge process; in particular, weak discharge processes are especially susceptible to information loss. In contrast, with the adoption of continuous acquisition, a higher trigger threshold could be set to prevent false triggering as long as a reasonable pretrigger time is chosen, thus allowing more complete lightning discharge information and, in turn, more complete positioning results to be obtained.

In addition to improvements in electric field detection equipment and signal acquisition modes, the station network layout adopted for the detection equipment also has a very important impact on the detection ability and channel positioning results achieved for lightning electric fields. The earliest established lightning detection station networks working in the LF/VLF band focused on the location and monitoring of the return strokes of ground flashes. The pulse signal of a ground flash return stroke is usually transmitted over quite a far distance, even hundreds of kilometers. Later, researchers found that the lightning discharge pulses in clouds can also be used for positioning and for the analysis of physical processes related to both thunderstorms in general and lightning in particular. Accordingly, the so-called total flash location systems, which can locate some of the discharge pulses occurring inside clouds and return stroke pulses, were developed. In general, the baseline lengths of the lightning detection systems intended for tracking lightning activity during large-scale thunderstorms

are typically long. The design and establishment of LFEDA also drew on the lessons learned from such station network layouts. However, although it has been found that electric field detection equipment operating in the LF/VLF band can also yield rich lightning channel information when appropriate signal processing methods are used to extract the location information carried by electric fields, the rapid attenuation with distance that occurs during electric field transmission greatly limits the potential exploitation of this location information. Due to rapid developments in electronic technology and the practical needs of lightning physics research, it is becoming necessary to meet increasingly stringent requirements in terms of fine lightning positioning based on the detection of lightning electromagnetic fields. Therefore, there is a need to develop lightning positioning systems based on electromagnetic field detection in the LF/VLF band with fine channel positioning capabilities. To this end, the station network baselines should be shortened as much as possible while maintaining distinguishable time differences.

In addition, for positioning systems operating in the LF/VLF band, it is also important to explore methods of improving the performance of signal processing and analysis to improve the ultimate lightning positioning capability. This is because the accuracy of the location information obtained through TOA-based lightning location techniques depends on the accuracy of electric field waveform matching and pulse peak time extraction. However, the LF/VLF electromagnetic field detection systems are highly complex and extremely susceptible to interference because of their relatively large bandwidth. Therefore, appropriate signal processing and analysis methods are very important, whether for signal quality control or for accurate extraction of key pulse information.

Improvements in LFEDA's positioning capabilities have been realized primarily on the basis of advancements in signal processing and positioning algorithms, motivated by the fact that it will not be possible to upgrade the performance of the existing detection equipment and station network layout for at least the next few years. Relative to the current signal analysis methods and the corresponding positioning capabilities of LFEDA, the DBM_EEMD algorithm proposed in this article is very effective in suppressing noise interference and greatly improves the ability to extract the weak electric field pulse signals generated during the lightning discharge process, thereby allowing more abundant lightning positioning information to be obtained. Hence, the algorithm is expected to play an important role in improving the lightning location ability from the perspective of signal analysis.

ACKNOWLEDGMENT

The authors would like to thank the Editors and the Anonymous Reviewers for their constructive comments and suggestions, which greatly helped them improve the technical quality and presentation of this article.

REFERENCES

[1] X. P. Fan et al., "A new method of three-dimensional location for low-frequency electric field detection array," J. Geophys. Res., Atmos., vol. 123, no. 16, pp. 8792–8812, Aug. 2018, doi: 10.1029/ 2017JD028249.

- [2] V. A. Rakov and M. A. Uman, Lightning: Physics and Effects. Cambridge, MA, USA: Cambridge Univ. Press, 2003.
- [3] X. Qie, D. Liu, and Z. Sun, "Recent advances in research of lightning meteorology," *J. Meteorolog. Res.*, vol. 28, no. 5, pp. 983–1002, Oct. 2014, doi: 10.1007/s13351-014-3295-0.
- [4] K. L. Cummins and M. J. Murphy, "An overview of lightning locating systems: History, techniques, and data uses, with an indepth look at the U.S. NLDN," *IEEE Trans. Electromagn. Compat.*, vol. 51, no. 3, pp. 499–518, Aug. 2009, doi: 10.1109/TEMC.2009. 2023450.
- [5] K. L. Cummins, M. J. Murphy, E. A. Bardo, W. L. Hiscox, R. B. Pyle, and A. E. Pifer, "A combined TOA/MDF technology upgrade of the U.S. National lightning detection network," *J. Geophys. Res.*, *Atmos.*, vol. 103, no. D8, pp. 9035–9044, Apr. 1998, doi: 10.1029/98JD00153.
- [6] C. J. Biagi, K. L. Cummins, K. E. Kehoe, and E. P. Krider, "National lightning detection network (NLDN) performance in Southern Arizona, Texas, and Oklahoma in 2003–2004," J. Geophys. Res., vol. 112, no. D5, 2007, Art. no. D05208, doi: 10.1029/2006JD007341.
- [7] A. Lafkovici, A. M. Hussein, W. Janischewskyj, and K. L. Cummins, "Evaluation of the performance characteristics of the North American lightning detection network based on tall-structure lightning," *IEEE Trans. Electromagn. Compat.*, vol. 50, no. 3, pp. 630–641, Aug. 2008, doi: 10.1109/TEMC.2008.927922.
- [8] L. Chen et al., "Comparative analysis between LLS and observation of artificial-triggered lightning," High Voltage Eng., vol. 35, pp. 1896–1902, Aug. 2009.
- [9] Y. Zhang et al., "A review of advances in lightning observations during the past decade in Guangdong, China," J. Meteorolog. Res., vol. 30, no. 5, pp. 800–819, Aug. 2016, doi: 10.1007/s13351-016-6928-7.
- [10] M. Azadifar et al., "Evaluation of the performance characteristics of the European lightning detection network EUCLID in the Alps region for upward negative flashes using direct measurements at the instrumented Säntis tower," J. Geophys. Res., Atmos., vol. 121, no. 2, pp. 595–606, Jan. 2016, doi: 10.1002/2015JD024259.
- [11] D. A. Smith, "The Los Alamos Sferic Array: A research tool for lightning investigations," J. Geophys. Res., vol. 107, no. D13, pp. ACL-5-1–ACL-5-14, Jul. 2002, doi: 10.1029/2001JD000502.
- [12] D. A. Smith et al., "A method for determining intracloud lightning and ionospheric heights from VLF/LF electric field records," Radio Sci., vol. 39, no. 1, Feb. 2004, Art. no. RS1010, doi: 10.1029/ 2002RS002790.
- [13] X.-M. Shao, M. Stanley, A. Regan, J. Harlin, M. Pongratz, and M. Stock, "Total lightning observations with the new and improved Los Alamos Sferic Array (LASA)," *J. Atmos. Ocean. Technol.*, vol. 23, no. 10, pp. 1273–1288, Oct. 2006, doi: 10.1175/JTECH1908.1.
- [14] P. M. Bitzer et al., "Characterization and applications of VLF/LF source locations from lightning using the Huntsville Alabama Marx meter array," J. Geophys. Res., Atmos., vol. 118, no. 8, pp. 3120–3138, Apr. 2013, doi: 10.1002/jgrd.50271.
- [15] M. Stolzenburg et al., "Strokes of upward illumination occurring within a few milliseconds after typical lightning return strokes," J. Geophys. Res., Atmos., vol. 117, no. D15, Aug. 2012, Art. no. D15203, doi: 10.1029/2012JD017654.
- [16] S. Karunarathne et al., "Locating initial breakdown pulses using electric field change network," J. Geophys. Res., Atmos., vol. 118, no. 13, pp. 7129–7141, Jul. 2013, doi: 10.1002/jgrd.50441.
- [17] S. Yoshida, T. Wu, T. Ushio, K. Kusunoki, and Y. Nakamura, "Initial results of LF sensor network for lightning observation and characteristics of lightning emission in LF band," *J. Geophys. Res., Atmos.*, vol. 119, no. 21, pp. 12034–12051, Nov. 2014, doi: 10.1002/2014JD022065.
- [18] Y. Wang et al., "Beijing Lightning Network (BLNET) and the observation on preliminary breakdown processes," Atmos. Res., vol. 171, pp. 121–132, May 2016, doi: 10.1016/j.atmosres.2015.12.012.
- [19] F. Lyu et al., "A low-frequency near-field interferometric-TOA 3-D lightning mapping array," Geophys. Res. Lett., vol. 41, no. 22, pp. 7777–7784, Nov. 2014, doi: 10.1002/2014GL061963.
- [20] F. Lyu, S. A. Cummer, G. Lu, X. Zhou, and J. Weinert, "Imaging lightning intracloud initial stepped leaders by low-frequency interferometric lightning mapping array," *Geophys. Res. Lett.*, vol. 43, no. 10, pp. 5516–5523, May 2016, doi: 10.1002/2016GL069267.
- [21] T. Wu, D. Wang, and N. Takagi, "Lightning mapping with an array of fast antennas," *Geophys. Res. Lett.*, vol. 45, no. 8, pp. 3698–3705, Apr. 2018, doi: 10.1002/2018GL077628.
- [22] N. Kitagawa and M. Brook, "A comparison of intracloud and cloud-to-ground lightning discharges," J. Geophys. Res., vol. 65, no. 4, pp. 1189–1201, Apr. 1960, doi: 10.1029/JZ065i004p01189.

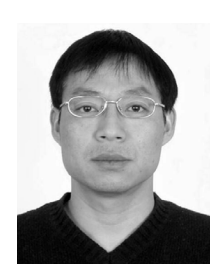
- [23] D. Shi et al., "Low-frequency E-field detection array (LFEDA)— Construction and preliminary results," Sci. China Earth Sci., vol. 60, no. 10, pp. 1896–1908, Oct. 2017, doi: 10.1007/s11430-016-9093-9.
- [24] N. E. Huang et al., "The empirical mode decomposition and the Hilbert spectrum for nonlinear and non-stationary time series analysis," Proc. Roy. Soc. London. A, Math., Phys. Eng. Sci., vol. 454, no. 1971, pp. 903–995, Mar. 1998, doi: 10.1098/rspa.1998.0193.
- [25] X. Fan, Y. Zhang, Q. Yin, Y. Zhang, and D. Zheng, "Characteristics of a multi-stroke 'bolt from the blue' lightning-type that caused a fatal disaster," *Geomatics, Natural Hazards Risk*, vol. 10, no. 1, pp. 1425–1442, Jan. 2019, doi: 10.1080/19475705.2018.1553800.
- [26] Z. Chen et al., "A method of three-dimensional location for LFEDA combining the time of arrival method and the time reversal technique," J. Geophys. Res., Atmos., vol. 124, no. 12, pp. 6484–6500, Jun. 2019, doi: 10.1029/2019JD030401.
- [27] N. E. Huang, Z. Shen, and S. R. Long, "A new view of nonlinear water waves: The Hilbert spectrum," *Annu. Rev. Fluid Mech.*, vol. 31, no. 1, pp. 417–457, Jan. 1999, doi: 10.1146/annurev.fluid.31.1.417.
- [28] G. Rilling, P. Flandrin, and P. Gonçalves, "On empirical mode decomposition and its algorithms," in *Proc. IEEE-EURASIP Workshop Nonlinear Signal Image Process. (NSIP)*, Grado, Italy, Jun. 2003, pp. 8–11.
- [29] N. E. Huang and Z. Wu, "A review on Hilbert-Huang transform: Method and its applications to geophysical studies," *Rev. Geophys.*, vol. 46, no. 2, Jun. 2008, Art. no. RG2006, doi: 10.1029/2007RG000228.
- [30] Z. Wu and N. E. Huang, "Ensemble empirical mode decomposition: A noise-assisted data analysis method," Adv. Adapt. Data Anal., vol. 1, no. 1, pp. 1–41, Jan. 2009, doi: 10.1142/S1793536909000047.
- [31] X. M. Shao, P. R. Krehbiel, R. J. Thomas, and W. Rison, "Radio interferometric observations of cloud-to-ground lightning phenomena in florida," *J. Geophys. Res.*, vol. 100, no. D2, pp. 2749–2783, Feb. 1995, doi: 10.1029/94JD01943.
- [32] W. Rison, R. J. Thomas, P. R. Krehbiel, T. Hamlin, and J. Harlin, "A GPS-based three-dimensional lightning mapping system: Initial observations in central New Mexico," *Geophys. Res. Lett.*, vol. 26, no. 23, pp. 3573–3576, Dec. 1999, doi: 10.1029/1999GL010856.
- [33] L. M. Coleman et al., "Effects of charge and electrostatic potential on lightning propagation," J. Geophys. Res., Atmos., vol. 108, no. D9, p. 4298, May 2003, doi: 10.1029/2002JD002718.
- [34] W. D. Rust et al., "Inverted-polarity electrical structures in thunderstorms in the severe thunderstorm electrification and precipitation Study (STEPS)," Atmos. Res., vol. 76, nos. 1–4, pp. 247–271, Jul. 2005, doi: 10.1016/j.atmosres.2004.11.029.
- [35] G. Zhang et al., "Using lightning locating system based on time-of-arrival technique to study three-dimensional lightning discharge processes," Sci. China Earth Sci., vol. 53, no. 4, pp. 591–602, Apr. 2010, doi: 10.1007/s11430-009-0116-x.
- [36] Y. Li et al., "Electrical structure of a Qinghai–Tibet plateau thunderstorm based on three-dimensional lightning mapping," Atmos. Res., vol. 134, pp. 137–149, Dec. 2013, doi: 10.1016/j.atmosres.2013.07.020.
- [37] D. Zheng et al., "Characteristics of the initial stage and return stroke currents of rocket-triggered lightning flashes in Southern China," J. Geophys. Res., Atmos., vol. 122, no. 12, pp. 6431–6452, Jun. 2017, doi: 10. 1002/2016JD026235.
- [38] Y. Zhang et al., "Observations of the initial stage of a rocket-and-wire-triggered lightning discharge," Geophys. Res. Lett., vol. 44, no. 9, pp. 4332–4340, May 2017, doi: 10.1002/2017GL072843.



Xiangpeng Fan received the B.S. degree in atmospheric sciences from Lanzhou University, Lanzhou, China, in 2008, the M.Sc. degree in atmospheric physics from the Cold and Arid Regions Environment and Engineering Research Institute, Chinese Academy of Sciences, Lanzhou, in 2011, and the Ph.D. degree in atmospheric sciences from the Chinese Academy of Sciences, Beijing, China, in 2019.

He is an Associate Professor with the State Key Laboratory of Severe Weather, Chinese Academy

of Meteorological Sciences, Beijing. His research interests include lightning physics and lightning detection.



Yijun Zhang received the B.Sc. degree in physics from Hebei Normal University, Hebei, China, in 1986, and the M.Sc. and Ph.D. degrees in atmospheric physics from the Cold and Arid Regions Environment and Engineering Research Institute, Chinese Academy of Sciences, Lanzhou, China, in 1989 and 1998, respectively.

He is a Professor with the Department of Atmospheric and Oceanic Sciences, Institute of Atmospheric Sciences, Fudan University, Shanghai, China. His research interests include atmospheric

electricity, lightning physics, and thunderstorm electricity.



Wen Yao received the M.S. degree in atmospheric sounding from the Nanjing University of Information Science and Technology, Nanjing, China. in 2001.

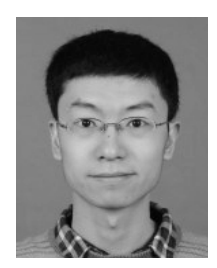
She is a Professor with the Chinese Academy of Meteorological Sciences, Beijing, China. Her research interests include the key technologies of meteorological observation instruments, the application of meteorological observational information, and severe weather forecasting.



Paul R. Krehbiel received the B.Sc. and M.Sc. degrees in electrical engineering (with a physics option) from the Massachusetts Institute of Technology, Cambridge, MA, USA, in 1963 and 1966, respectively, and the Ph.D. degree in physics from the University of Manchester Institute of Science and Technology, Manchester, U.K., in 1982.

He is a Professor of physics with the Physics Department and Langmuir Laboratory for Atmospheric Research, New Mexico Institute of

Mining and Technology, Socorro, NM, USA.



Liangtao Xu received the B.S. degree in atmospheric sciences from Sun Yat-Sen University, Guangzhou, China, in 2009, and the Ph.D. degree in meteorology from the Chinese Academy of Sciences, Beijing, China, in 2015.

In 2015, he joined the State Key Laboratory of Severe Weather, Chinese Academy of Meteorological Sciences, Beijing, as an Assistant Professor. Since 2018, he has been an Associate Professor. He is involved in research on numerical weather predictions and cloud physics.



Yang Zhang received the Ph.D. degree in physical electronics from the Chinese Academy of Sciences, Beijing, China, in 2008.

He is a Professor with the State Key Laboratory of Severe Weather, Chinese Academy of Meteorological Science, Beijing. His research interests include thunderstorm detection, lightning location, and lightning physics.



Hengyi Liu was born in Hebei, China, in 1981. He received the B.Sc. degree from Hebei University, Hebei, China, in 2004, and the Ph.D. degree from the Chinese Academy of Sciences, Beijing, China, in 2012.

He is an Associate Professor with the State Key Laboratory of Severe Weather, Chinese Academy of Meteorological Sciences, Beijing. His research interests include lightning physics and lightning detection.



Dong Zheng received the B.S. degree in atmospheric sciences from Lanzhou University, Lanzhou, China, in 2002, and the M.S. and Ph.D. degrees in atmospheric sciences from the Chinese Academy of Sciences, Beijing, China, in 2005 and 2008, respectively.

Since 2016, he has been a Professor with the State Key Laboratory of Severe Weather, Chinese Academy of Meteorological Sciences, Beijing. He has authored more than 100 articles. His research interests include thunderstorm and lightning, severe

weather, lightning detection, lightning physics, and lightning warning and forecasting.



Weitao Lyu received the Ph.D. degree in atmospheric physics from the University of Science and Technology of China, Hefei, China, in 2003.

He is a Professor with the Chinese Academy of Meteorological Science, Beijing, China. His research interests include lightning physics, lightning detection, and lightning protection.